

Experimental study on pion capture by hydrogen bound in molecules*

D. Horváth,[†] K.A. Aniol,[‡] F. Entezami, D.F. Measday, A.J. Noble, S. Stanislaus,
and C.J. Virtue,[§]

Department of Physics, University of British Columbia, Vancouver, B.C., Canada V6T 2A6

A.S. Clough, D.F. Jackson, J.R.H. Smith[¶]

Department of Physics, University of Surrey, Guildford, U.K.

M. Salomon,

TRIUMF, Vancouver, B.C., Canada V6T 2A3,

Abstract

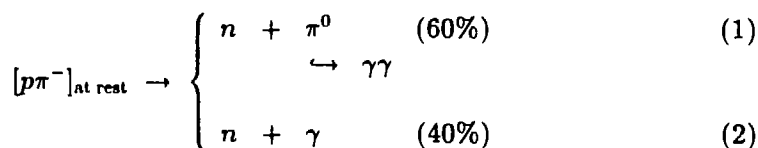
An experiment was performed at TRIUMF to study the formation of pionic hydrogen atoms and molecules in solids, particularly in groups of organic molecules of slightly different structure in order to help further clarify the problem. The nuclear capture of pions by hydrogen was measured using the charge exchange of stopped pions. The coincident photons emitted by the decaying π^0 mesons were detected by TRIUMF's two large NaI spectrometers. New experimental results were obtained for the capture probability of stopped π^- mesons in the nuclei of hydrogen atoms, chemically bound in molecules of some simple hydrides, acid anhydrides, and sugar isomers. A linear relation was found between pion capture in hydrogen and melting point in sugar isomers. The pion capture probability in acid anhydrides is fairly well described by a simple atomic capture model in which the capture probability on the hydrogen dramatically increases as the hydrogen atom is separated from the strongly electronegative C_2O_3 group. Both effects are consistent with a correlation between pion capture and electron density on hydrogen atoms.

(submitted to Physical Review A)

I. INTRODUCTION

Pionic hydrogen ($p\pi^-$) is an exotic atom which has many unusual properties and whose formation and decay mechanisms are not fully understood. The possible use of this atom for obtaining physico-chemical information was first suggested by Petrukhin, Ponomarev, and Prokoshkin,¹ and most of the experimental measurements to date have been made at Dubna. The topic has been reviewed several times,²⁻⁴ and we refer the reader to those articles for a detailed discussion of the various experiments and the conclusions that have been drawn.

In most studies, all that is observed is the strong absorption of the pion on the proton,



following the slowing down and atomic capture of a π^- . Since π^0 -production at rest is unique to hydrogen (except for ${}^3\text{He}$ (Ref. 5)), the decay of the π^0 is an unambiguous signal that the π^- has reached a low energy orbit in hydrogen. Thus when a π^- is stopped in any material, it is possible to identify whether it is captured by hydrogen. Using π^- -mesic X-rays one can study pion capture on other nuclei, so the methods complement each other. In addition, μ^- -capture is very similar and X-ray studies or the lifetime technique can be used to obtain related information.

The capture of the π^- and the subsequent cascade down to a tightly bound orbit constitute a complicated series of events (Fig. 1), yet the experiment measures only one parameter, viz. the probability that the π^- is captured by the proton of the hydrogen nucleus. It is thus very difficult to specify what happens in any detail, and there is still a significant disagreement about the relative importance of various mechanisms in the cascade. A reasonable way to obtain useful information is to choose a variety of chemical systems and to try to find patterns of behaviour for the capture process.

The capture of the π^- in the molecule occurs at relatively low kinetic energies between 10 eV and 1 keV. The π^- enters the molecule by ejecting electrons and thereby losing more energy. When the π^- is eventually absorbed on the proton, it is known that the $p\pi^-$ atom has a kinetic energy of a few eV (Ref. 6). This is determined from the width of the energy for the recoiling neutron in the charge-exchange reaction $p\pi^- \rightarrow n\pi^0$.

It turns out that the Auger process of the Coulomb-capture is very important and is sensitive to small differences in the electron wave function. This sensitivity is found in μ^- -capture as well. Whether the π^- is absorbed by the proton or not depends significantly on the electron distribution around the proton in the molecule, i.e. on the chemical bond properties of the hydrogen. This relationship has been demonstrated in great detail by the measurements of Petrukhin *et al.* on various

chemical systems: viz. acids and bases, aliphatic and aromatic organic compounds, metal and nonmetal hydrides, aquacomplexes and aqueous solutions.²⁻⁴

One of the key observations is that pion capture on the hydrogen is very different in hydrazine (N_2H_4) and in a gaseous mixture of the same composition. In hydrazine the pion capture probability is suppressed by a factor of 30 (Ref. 2):

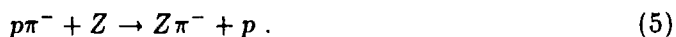
$$W(N_2 + 2H_2)/W(N_2H_4) \approx 30 . \quad (3)$$

Similarly, there is a difference between pion capture in HD and $H_2 + D_2$ (Ref. 7):

$$W(H_2 + D_2)/W(HD) = 1.23 \pm 0.03 . \quad (4)$$

To explain this dramatic sensitivity Ponomarev proposed the *large mesic molecule* (LMM) model.³ It is postulated that the π^- ejects a molecular electron (with a probability P in Fig. 1) and replaces it in an orbit which is large for the pion and thus highly excited. There being no Pauli principle for the π^- it can then de-excite. At this stage several mechanisms may come into play:

a) The π^- can detach itself from the molecule in the form of a small, fast and neutral $p\pi^-$ atom (with a probability Q) and then be captured by the proton (probability R) or suffer transfer to another atom in a collision (probability $1 - R$):



b) The π^- can preferentially select the higher Z atoms of the molecule directly.

c) In addition, it was suggested^{8,9} that the π^- can first form a $p\pi^-$ atom directly (probability D) and then get transferred to another atom of the same molecule by tunnelling ("internal" transfer).

According to the original LMM model the probability that the pion is captured on the proton (W) can be described as

$$W = P \times Q \times R \quad (6)$$

where P is the formation probability of a $Zp\pi^-$ molecule, Q is the probability that the pion undergoes transition from the molecular to a $p\pi^-$ atomic state and R is the probability that from the pionic hydrogen ($p\pi^-$) the pion will be absorbed on a proton (but not necessarily on the initial proton) and not transferred to a heavier nucleus. The probability for direct capture from the molecular orbit (E in Fig. 1) was assumed to be zero. As emphasized above, the experiment measures only W , so the relative values of P , Q , and R have to be deduced indirectly from comparative measurements in related materials.

From the various experiments it is well known that external transfer is certainly a major factor in certain chemical systems, for example in mixtures of H_2 + noble gases,¹⁰ as well as H_2 + heavy molecules,¹¹ or CH_2 + noble gases.¹² Collisional transfer can reduce the $p\pi^-$ capture probability by a factor of 5 to 10 and thus it may significantly contribute to the suppression of the W probability.

At this point we should issue one word of warning. A recent experiment by Bannikov *et al.*¹³ ^3He with various gases. This is an important case because a π^- is very unlikely to be transferred once it is captured by ^3He . It was also a convenient probe because the same technique of π^0 detection could be used, π^- charge exchange having a branching ratio of 13% for $^3\text{He} \pi^-$ at rest.^{13,14} Thus the observation of π^0 production is sensitive to the initial capture process only. They showed that the probability for capture is not directly proportional to the slowing-down power of the medium. This is serious because a lot of earlier Dubna experiments had made this implicit assumption; for example, a key experiment on transfer in liquids is thus undermined¹⁵ and the effect needs to be reconfirmed. It is important to note that this difference between slowing down and capture refers to slowing down at relatively high energies (≥ 1 keV). There does *not* appear to be any difference between the slowing-down power and capture at the low energies for which capture occurs. Thus there is no concentration dependence of the atomic capture ratio in the experiment of Bannikov *et al.* This confirms many earlier experiments with μ^- , for example in different mixtures of alkali halides¹⁶ or in Nb/V alloys, where Nb/V atomic ratio was varied from 0.046 to 18.5 (Ref. 17). In all these cases the capture ratio was found to be independent of concentration.

Because of these conundrums, there have been renewed discussions of the capture process. Jackson *et al.* emphasized the dynamics of π^- capture within the molecule.^{8,9} Unfortunately, it is very difficult to unravel these details experimentally because all that is observed is the final result. Another approach has been that of Daniel *et al.*¹⁸ who observed that transfer alters the higher Lyman transitions in muonic atoms. They claim that there is no evidence for meson molecule formation, but they do not offer an explanation for the enormous suppression (3) of $p\pi^-$ capture in hydrazine compared to $\text{H}_2 + 2\text{N}_2$. A theoretical study of pion molecular orbitals¹⁹ indicates that mesomolecular formation can occur but may be less important than is usually implied by the molecular model. This work also shows that the tunnelling mechanism can explain the transfer of pions from hydrogen to heavier atoms in the same molecule (internal transfer), hence causing suppression of the pion charge exchange reaction.

The present experiment was proposed at TRIUMF using equipment which had already demonstrated a very high sensitivity to π^0 production at rest.⁵ A preliminary account of these measurements has already appeared in a conference proceedings²⁰ and an extensive interpretation of the results of the preliminary analysis has already²¹ been published. The present analysis is slightly improved, so the experimental results are a little different, but these differences do not change our conclusions in any way. This paper will also give much more detail on the experimental method and the way the analysis proceeded.

II. EXPERIMENTAL TECHNIQUE

The experimental set-up is depicted in Fig. 2. The negative pion beam was stopped in the target after being slowed down by the plastic scintillators of beam counters S_1 , S_2 , and S_3 , and a graphite wedge degrader D ($\rho = 1.64 \text{ g/cm}^3$) of variable thickness. The beam had an initial momentum of $150 \text{ MeV}/c$ ($T_\pi = 65 \text{ MeV}$) and so had a total range of $\approx 16 \text{ g/cm}^2$ in carbon. The stopping was checked by veto counter S_4 . To reduce the π^0 background the scintillators of S_3 and S_4 were made of fully deuterated plastic (prepared by C. Hurlbut, BICRON, Inc.). For measuring the γ - γ coincidences from reaction (1) two large NaI(Tl) detectors, TINA ($\phi 46 \text{ cm} \times 51 \text{ cm}$) and MINA ($\phi 36 \text{ cm} \times 36 \text{ cm}$) were placed in steel shielding boxes with lead collimators (30.5 cm and 25.4 cm, respectively) at 80 cm and 70 cm from the target, opposite each other, each at a 90° angle to the beam line. Both NaI spectrometers were equipped with seven phototubes each. Thin (3.2 mm) plastic scintillation counters, S_5 and S_6 , covered the front faces of the NaI detectors behind the collimators to identify and reject the charged particles coming from the target (mostly electrons from photon conversion in the surrounding material: target holder, shielding, etc.).

The Dubna group used total-absorption lead glass Čerenkov counters for detecting the π^0 photons.² As the Čerenkov counters are insensitive to neutrons they could be placed very close to the target, allowing for a highly efficient detection of the hard ($54.9 \text{ MeV} \leq E_\gamma \leq 83.0 \text{ MeV}$) photons with a fairly sharp timing of the coincidences and a low sensitivity for the neutron and low-energy γ background. However, the large solid angle of the Čerenkov radiators made the pion charge exchange in flight the dominant source of the background.

The superiority of our method can be clearly demonstrated by comparing the branching ratios of the charge exchange of stopped π^- mesons in various heavy nuclei as measured with the two methods. The Dubna method provided a limit²² of <2 to 10×10^{-5} for the studied nuclei which was later reduced by a factor of two.⁴ Using NaI detectors at a sufficiently large distance from the target to measure time of flight to reject the neutrons, decreased the above limit down to <1 to 5×10^{-6} (Ref. 5), i.e. by an order of magnitude.

For data acquisition a PDP-11/34 computer was used with the MULTI²³ program package. A valid event was defined as a π^- -stop \cdot TINA \cdot MINA coincidence, i.e. $S_1 \cdot S_2 \cdot S_3 \cdot \bar{S}_4 \cdot$ TINA \cdot MINA. The events with a charged particle detected by TINA or MINA ($S_5 \cdot$ TINA or $S_6 \cdot$ MINA) were rejected during the off-line analysis.

The experiment was performed on the M11 pion channel at TRIUMF; the beam intensity was 1 to $2 \times 10^6 \text{ s}^{-1}$, $\sim 10\%$ of the beam flux was stopped in the target. The beam composition was checked by measuring the stop time of the beam particles with respect to the rf signal of the cyclotron by triggering events with random coincidences of $S_1 \cdot S_2 \cdot S_3 \cdot \bar{S}_4$ with a pulse generator. The stopped beam consisted of $89\% \pi^-$, $10\% \mu^-$, and $1\% e^-$. (For the incoming beam only about 50% of the particles were pions.) During the measurement the power supply of one of our bending magnets was unstable. We continuously checked the magnetic field using an NMR probe and manually kept the field stable. Also, a standard polyethylene target was regularly

measured for additional control and possible off-line correction.

III. SAMPLES

For this first *pion chemistry* experiment at TRIUMF we have chosen samples to establish the relation to the previous data (simple binary hydrides) and the following organic molecules to study chemical structure effects:

- Cyclic acid anhydrides to measure changes in $p\pi^-$ capture probabilities in molecules which differ by only one hydrocarbon group in the presence of a strong electrophilic group;
- Sugar isomers to find if differences suggested earlier on the basis of pionic X-ray studies of organic compounds⁸ are present in pion capture by hydrogen.
- Nitrogen compounds to study N-H bonds.

As our method is selectively sensitive to hydrogen, low-level (<1%) impurities do not affect the results. The organic compounds were analyzed for impurities using microanalysis after the run and none was found. It should be noted, however, that this method is insensitive to excess water content of the samples as that would be eliminated before elemental measurements were made.

All our samples were powdered solids except the citraconic anhydride which was a liquid. According to the available amount of the sample material we used targets of three different sizes:

- *LiH* and *urea* were kept in 102 mm ϕ \times 25.4 mm vessels with thin copper windows, made air-tight by teflon flanges.
- The *metal hydrides*, *methylsuccinic* and *citraconic anhydrides* were measured in 70 mm ϕ \times 15 mm aluminium boxes of 0.05 mm wall thickness (equivalent to 0.011 g/cm² of carbon) sealed by teflon tape on the outside.
- For the rest of the samples we used the aluminium boxes with a 67% increased volume (70 mm ϕ \times 25 mm).

For calibration, polyethylene samples were measured in every actual target holder and geometry.

IV. DATA ANALYSIS

The $b(E)$ energy distribution of the particle beam was determined by measuring range curves in LiH and polyethylene targets using the wedge degrader (D in Fig. 2). If one converts the pion energy E_π into a corresponding penetration depth (range)

D in units of g/cm^2 graphite, the fraction of pions stopping in the last beam counter S_3 , in target T and the veto counter S_4 can be described as

$$N_3 = N_0 \int_R^{R+\Delta_3} b(D)dD = N_0 \int_0^{\Delta_3} b(R+D)dD \quad (7)$$

$$N_T = N_0 \int_0^{\Delta_T} b(R+\Delta_3+D)dD \quad (8)$$

$$N_4 = N_0 \int_0^{\Delta_4} b(R+\Delta_3+\Delta_T+D)dD \quad (9)$$

where N_0 is the number of incoming π^- -mesons, R , Δ_3 , Δ_T , and Δ_4 are the thicknesses of the degrader, S_3 , the target, and S_4 , all in units of g/cm^2 of carbon.

Range curves were measured in the beginning and at the end of the experiment by counting the π^0 yield from a LiH and a polyethylene target as a function of the degrader thickness R (Fig. 3). The beam energy distribution had a Gaussian shape,

$$b(D) = \frac{1}{\sigma\sqrt{2\pi}} \exp\left(-\frac{[D-R_0]^2}{2\sigma^2}\right), \quad (10)$$

thus the measured range curves could be reasonably well fitted with the function

$$f(R) = \int_0^\infty b(D+R)dD = \frac{1}{2} \left[\operatorname{erf}\left(\frac{R+\Delta_T-R_0}{\sigma\sqrt{2}}\right) - \operatorname{erf}\left(\frac{R-R_0}{\sigma\sqrt{2}}\right) \right] \quad (11)$$

where

$$\operatorname{erf}(x) = \frac{2}{\sqrt{\pi}} \int_0^x e^{-t^2} dt \quad (12)$$

is the usual error function.

A typical range curve measured with our standard polyethylene target ($\Delta_T = 2.05 \text{ g}/\text{cm}^2$ of carbon) is shown in Fig. 3 together with the fitted function. All fitting procedures were performed using the CERN MINUIT program.²⁵ The experiment had two parts, the widths of the beam energy distribution were $\sigma_1 = (0.78 \pm 0.06) \text{ g}/\text{cm}^2$ of carbon in the first part and $\sigma_2 = (0.73 \pm 0.04) \text{ g}/\text{cm}^2$ of carbon in the second one. As we had an energy spread of $1.8 \text{ g}/\text{cm}^2$ of carbon full width at half maximum, we stopped only about 50% of the pions which reached S_3 in the target.

If a π^- -meson, stopped in target T, is captured by hydrogen (i.e. a free proton) the detected π^0 yield will be

$$N_{\pi^0}^T = \epsilon_T \omega W_T N_{\text{stop}}^T \quad (13)$$

where ϵ_T is the efficiency of π^0 detection from target T, $\omega = 60\%$ is the branching ratio of reaction (1), W_T is the capture probability of stopped π^- mesons by hydrogen in target T, and N_{stop}^T is the number of π^- -stops in the target.

N_{stop}^T can be determined using the following considerations. The number of pions disappearing between S_3 and S_4 is the sum of the π^- -stops in S_3 , the T sample, and the front and back walls of the target vessel:

$$N_{123\bar{4}} = N_{123} \kappa_3 + \epsilon_g N_{123} (\kappa_{FW} + \kappa_T + \kappa_{BW}) \quad (14)$$

where κ_3 , κ_{FW} , κ_T , and κ_{BW} are the fractions of pions stopped in S_3 , in the front wall, in the target, and in the back wall, respectively, $N_{123\bar{4}}$ and N_{123} are the numbers of $S_1 \cdot S_2 \cdot S_3 \cdot \bar{S}_4$ and $S_1 \cdot S_2 \cdot S_3$ coincidences, and ϵ_g is a geometric factor: the fraction of the beam (as represented by N_{123}) hitting the solid angle of the target. We can calculate the κ_x fractions from the known range curve using the corresponding equivalent thicknesses²⁸ as in Eqs. (7-9), and then ϵ_g from (14):

$$\epsilon_g = \frac{N_{123\bar{4}}/N_{123} - \kappa_3}{\kappa_{FW} + \kappa_T + \kappa_{BW}}. \quad (15)$$

Using (14) and (15) the number of π^- -stops in the target

$$N_{\text{stop}}^T = N_{123\bar{4}} - N_{123} \frac{\kappa_3 \times \kappa_T}{\kappa_{FW} + \kappa_T + \kappa_{BW}} - N_{123\bar{4}} \frac{\kappa_{FW} + \kappa_{BW}}{\kappa_{FW} + \kappa_T + \kappa_{BW}}. \quad (16)$$

The corrections introduced by the second and third terms of Eq. (16) are about 3% and 1%, respectively.

The π^0 yields were determined using the NaI time-of-flight and energy spectra. The time-of-flight (TOF) is defined by the time elapsed between the π^- stop in the target and the detection of the neutral particle by one of the NaI spectrometers. Figure 4 shows the two-dimensional distribution of TOF to TINA vs. TOF to MINA. The sharp peak in the lower left corner represents the γ - γ coincidences and the box shows the cuts applied in the off-line analysis.

Figure 5 demonstrates the effect of the various subsequent restrictions on the TINA energy spectrum. When a π^- stop is the only requirement (Fig. 5a) we can barely see the " π^0 box" between 54 and 83 MeV and the radiative capture peak at 129 MeV on top of the neutron background. The latter is mostly removed by the TOF cut (Fig. 5b). Finally, when we impose a condition that MINA detect a photon as well, only the minimal and maximal energy (54.9 MeV and 83.0 MeV) π^0 photons remain (Fig. 5c) corresponding to the π^0 mesons going towards MINA and TINA, respectively. Due to the similar solid angles for the two detectors, we have two peaks of roughly equal area in the photon energy spectra for each of the two NaI spectrometers.

The possible backgrounds of our photon energy spectra may be due to (a) random coincidences; and (b) π^- charge exchange in flight. The (a) random background should have a uniform energy distribution, while the in-flight π^0 -background will have an energy dependence similar to Fig. 5c, but broadened slightly.

In the course of the analysis the peaks in the measured energy spectra were approximated using an asymmetric function, sometimes called *NaI response function*

$$r(E_\gamma; B, C, D) = \frac{\left[1 - \operatorname{erf}\left(\frac{E_\gamma - B}{C}\right)\right] \exp\left(\frac{E_\gamma - B}{D}\right)}{2D \exp\left(\frac{C^2}{4D^2}\right)} \quad (17)$$

where E_γ is the measured photon energy, B , C , and D are adjustable parameters related to the location and left and right widths of the peak. As function r is normalized to unit area for any given target each of the π^0 photon energy spectra observed

by TINA or MINA can be fitted by two peaks of type (17) and a random background. This means 4×3 peak parameters, 1 area, and 2 background parameters for every target. We can make, however, a reasonable assumption that for our targets of roughly similar equivalent thicknesses, the peak shapes in the π^0 γ -energy spectra should be identical. Thus we can fit several spectra simultaneously²⁶ using the same peak shape parameters but individual area and background ones.

The fitting of the π^0 γ -energy spectra has shown the absence of any random background throughout the experiment. Thus, we could use the sum of counts under the measured curves as the π^0 -yield $N_{\pi^0}^T$, rather than the fitted area parameter. The W_T probability of capture of a stopped π^- in a hydrogen nucleus from Eq. (13) is

$$W_T = \frac{N_{\pi^0}^T}{\epsilon_T \omega N_{\text{stop}}^T}. \quad (18)$$

We still have to determine the ϵ_T efficiency of π^0 detection from target T . A computation using the method of intersecting cones⁵ has yielded $\epsilon_T \approx 2 \times 10^{-3}$ for the geometry of Fig. 2 with a point-like target. Although the absolute W_T values obtained with the above ϵ_T were quite close to the earlier results, due to the instability of our π^- beam we had to renormalize our data to those for a regularly measured polyethylene target. Thus the results presented in Table I are obtained by the formula

$$W_T = K_T \times \frac{\overline{W}_{\text{CH}_2}}{\overline{K}_{\text{CH}_2}} \quad (19)$$

where $K_T = N_{\pi^0}^T / N_{\text{stop}}^T$, and $\overline{K}_{\text{CH}_2}$ is $N_{\pi^0}^{\text{CH}_2} / N_{\text{stop}}^{\text{CH}_2}$ averaged over the polyethylene measurements before and after that of target T . As a normalization factor we accepted the average result of three independent absolute measurements²⁹⁻³¹ which is $\overline{W}_{\text{CH}_2} = 0.0129 \pm 0.0018$ (N.B. The relative result $\overline{W}_{\text{CH}_2} = 0.0145 \pm 0.0004$ (Refs. 4 and 27) was not included in the average.) We did *not*, however, include the error of $\overline{W}_{\text{CH}_2}$ in our errors, so that in the case of a later, more precise measurement of W_{CH_2} our results could be easily renormalized. For most of our targets we made two independent measurements and obtained W_T values which were always consistent; in Table I we present the weighted averages.

In order to check the π^0 background we repeatedly measured pure graphite targets which should yield no π^0 -mesons from stopped negative pions.⁵ We have detected some π^0 background in carbon, probably from hydrogen contamination of the environment and π^- charge exchange in flight. Note that this experiment used a much higher incident π^- -energy than the previous measurement.⁵ The present background corresponded to $W_C = (5.9 \pm 1.3) \times 10^{-5}$, and was subtracted from our measured W_T values. (There was a typographical error in our preliminary results.²⁰ The value for carbon, given as $(0.47 \pm 0.03) \times 10^{-3}$, should have read $(0.047 \pm 0.003) \times 10^{-3}$.) This was not done for our preliminary results²⁰; the present values are, therefore, slightly lower.

V. RESULTS AND DISCUSSION

Table I presents our data: sample name, target thickness in units of carbon equivalent i.e. $\text{g}/\text{cm}^2 \text{C}$, the detected π^0 yield, and the W_T probability from Eq. (18) after background subtraction. The chemical structures of some of the molecules are illustrated in Fig. 6. As mentioned earlier, we had two runs, and some of our samples were measured in both with a good reproducibility of the results. The thicknesses of our targets varied between 1.0 and 2.5 $\text{g}/\text{cm}^2 \text{C}$. One of our possible sources of systematic error is target size. We checked our method for such an effect on CH_2 samples of different thicknesses and found an $(11 \pm 5)\%$ reduction when reducing the target thickness from 1.8 to 0.85 $\text{g}/\text{cm}^2 \text{C}$. We did not correct our results for this effect which probably comes from an error in determining the beam energy distribution parameters from the range curve.

The LiH and CaH_2 measurements gave results compatible with previous measurements (see Table II) but that for niobium hydride is quite different. This sample has a W_T value close to the sensitivity limit of the Dubna method. None of the other materials have been measured before.

Five hexose and two pentose isomers of sugar have been measured. The pentose isomer, L-arabinose, was the only L-isomer measured, all others being D-isomers. Three of the sugar isomers, D(+)-galactose, α -D-glucose, and β -D-fructose, were specified as being anhydrous, the others carried a caution that they *might* not be anhydrous. The measured pion capture rates in hydrogen, W_T , for the sugars ranged from $(1.573 \pm 0.067) \times 10^{-3}$ to $(1.897 \pm 0.072) \times 10^{-3}$ giving a range of 5 standard deviations, rather large to be statistical. These W_T values can be compared with each other without any model calculation or renormalization as all of our sugar isomers have the same atomic composition H:C:O = 2:1:1. A linear relationship was found between the melting points of the anhydrous sugar isomers and the measured W_T values (see Fig. 7). Note that the melting point of β -D-glucose sensitively depends on its excess water content, and can be as low as 86°C in a hydrous state; this might be the reason why it deviates from the rest. As the variation of the melting point for these isomers is dominantly determined by the presence and strength of the hydrogen bonds among the molecules, the relationship of Fig. 7 is consistent with a greater degree of hydrogen bonding causing a higher melting point and reducing the electron density around the hydrogen atoms and hence reducing the pion capture probability by hydrogen. The latter effect of hydrogen bonds on pion capture was found in water³³ and ammonia.³⁴

In the event only three nitrogen compounds were measured. The large difference between uric acid ($W_T = (0.172 \pm 0.022) \times 10^{-3}$) and urea ($W_T = (1.334 \pm 0.058) \times 10^{-3}$) is consistent with the reduction effect of acidity on pion capture found earlier.³⁵

The results for acid anhydrides show a general increase in W_T , with increasing number of hydrogen atoms per molecule. This is, of course, consistent with the concentration dependence mentioned in the introduction. We made an attempt to fit the anhydride data using the simplest possible phenomenological model, by accounting for the individual pion capture contributions of the atoms in various positions. We

assume that the rate for absorption on a particular atom varies with its position in the molecule. Each anhydride has a strongly electronegative C_2O_3 group, and its rate for pion capture will be normalized to unity. In addition we have single and double bonded carbon atoms (with absorption rates C^S and C^D) and hydrogen atoms on double bonded carbon (H^0) or on single bonded carbon, 1, 2, or 3 C-C bond lengths away from the C_2O_3 group (H^1 , H^2 , and H^3). Thus, for example, the probability for capture by hydrogen in glutaric anhydride (see Fig. 6) is

$$W_H = \frac{4H^1 + 2H^2}{1 + 3C^S + 4H^1 + 2H^2}.$$

The least-squares fitting²⁵ gave the results presented in Tables III and IV. Surprisingly enough, the pion capture contributions of both kinds of carbon atoms came out to be negligibly small, while those of the hydrogen atoms were monotonically increasing with increasing distance from the electronegative C_2O_3 group. It is highly unlikely that C^S or C^D are really zero. To test the sensitivity of the hydrogen parameters to the absorption rate in carbon in fit 2 we set $C^S = 1.6 \times 10^{-3}$ and $C^D = 28.7 \times 10^{-3}$, i.e. the error band of the free fit. We see (Table III) that the numerical values of the H^n parameters are not sensitive to the carbon rates. Similarly in fit 3 we set $C^S = C^D = 20 \times 10^{-3}$. Apparently, there is not enough information in our data set to estimate the capture rates in carbon atoms, while the hydrogen contributions seem to be fairly well determined.

It is clear that the pion capture rate in hydrogen substantially increases when the hydrogen atom is further away from the C_2O_3 group. This observation is consistent with the earlier evidence on the relation between the presence of electronegative groups in hydrogenous molecules and the reduction of pion capture probability on hydrogen.^{36,37} Those groups distort the electron distribution in the molecule by attracting excess electrons from other atoms. This apparent positive charge is then shared by the atoms of the rest of the molecule according to their respective electronegativities and, in the case of a linear molecule such as the anhydrides, their distances from the electronegative group.³⁸ Thus the observed differences of pion capture on hydrogen are due to differences in electron density distribution in the molecule, as shown in the theoretical calculations of Tranquille and Jackson.¹⁹ The observed differences in pion capture probability are generally much higher than the estimated changes in electron density, as is discussed in detail by Tranquille and Jackson. Another striking example is the factor of 2 increase in pion capture on hydrogen, observed in Dubna, when water was heated to supercritical temperatures, while the calculations predict a ~10% increase in electron density on hydrogen due to the destruction of hydrogen bonds.³³

There is another possible explanation or contribution to the observed effect in the anhydrides: collisional pion transfer from the $p\pi^-$ atom to the C_2O_3 group within the same molecule. When the $p\pi^-$ is ejected, it can collide with the nearby atoms; that is how it most probably loses its excitation energy. When the $p\pi^-$ is formed near the C_2O_3 group, the higher Z of oxygen could be a strong trap, so the $p\pi^-$ may collide with the groups with a higher probability and hence it will produce π^0 mesons with a

lesser efficiency. However, the electron density effect is, probably, the dominant one; the difference between H^0 and H^1 , e.g., cannot be explained by transfer only.

VI. CONCLUSION

Using TRIUMF's high-resolution NaI γ -spectrometers we have studied the nuclear capture of stopped π^- mesons in chemically bound hydrogen by detecting the coincident photons emitted by the decaying π^0 -mesons from charge-exchange at rest. Metal hydrides, sugar isomers, acid anhydrides and nitrogen compounds were studied. For the metal hydrides we established a reasonable agreement with the results of previous pion capture experiments. The nitrogen compounds exhibit the acidity effect observed earlier. We found an interesting new relation between pion capture and molecular structure, namely a linear relationship between the W_T pion capture probability and the melting point of sugar isomers with the same chemical composition. The W_T values measured in acid anhydrides can be fairly well described in terms of a simple, phenomenological atomic capture model, in which the capture probability on the hydrogen increases as the hydrogen atom is separated from the avaricious C_2O_3 group. The results are in agreement with the concept that pion capture on hydrogen is related to the electron density of the hydrogen atom in the molecule, and confirm the earlier observation that those hydrogen atoms bound to or near carbon atoms with double bonds capture pions with a lower efficiency. At the same time, however, they suggest that the carbon atoms have a negligible role in pion capture in acid anhydrides. This effect is probably an artefact caused by errors and our particular choice of targets, but it is worth investigating further.

References

*Work supported by NSERC (Canada) and SERC (U.K.).

[†]On leave from Central Research Institute for Physics, H-1525 Budapest, Hungary.

[‡]Present address: Dept. of Physics & Astronomy, California State Univ., Los Angeles.

[§]Present address: NRC, Physics Dept., Carleton University, Ottawa, Canada K1S 5B6.

[¶]Present address: Daresbury Laboratory, Warrington, WA44AD, UK.

¹V.I. Petrukhin, L.I. Ponomarev, and Yu.D. Prokoshkin, *Khim. Vys. Energ. (USSR)* **1**, 283 (1967).

²S.S. Gerstein, V.I. Petrukhin, L.I. Ponomarev, and Yu.D. Prokoshkin, *Usp. Fiz. Nauk (USSR)* **97**, 3 (1969); *Sov. Phys. Uspekhi* **12**, 1 (1970).

³L.I. Ponomarev, *Annu. Rev. Nucl. Sci.* **23**, 395 (1973).

⁴D. Horváth, *Radiochim. Acta* **28**,241 (1981); *Hyperfine Interactions* **17-19** 679 (1984).

⁵B. Bassalleck, F. Corriveau, M.D. Hasinoff, T. Marks, D.F. Measday, J.-M. Poutissou, and M. Salomon, *Nucl. Phys.* **A362**, 445 (1981).

⁶J.F. Crawford, M. Daum, R. Frosch, B. Jost, P.-R. Kettle, R.M. Marshall, and

- K.O.H. Ziock, Phys. Rev. Lett. **56**, 1043 (1986). Also J.F. Crawford, M. Daum, R. Frosch, B. Jost, P.-R. Kettle, R.M. Marshall, B.K. Wright, and K.O.H. Ziock, PSI preprint PR-88-05.
- ⁷K.A. Aniol, D.F. Measday, M.D. Hasinoff, H.W. Roser, A. Bagheri, F. Entezami, C.J. Virtue, J. Stadlbauer, D. Horváth, M. Salomon, and B.C. Robertson, Phys. Rev. A **28**, 2684 (1983).
- ⁸D.F. Jackson, C.A. Lewis, and K. O'Leary, Phys. Rev. A **25**, 3262 (1982).
- ⁹D.F. Jackson, Phys. Lett. **95A**, 487 (1983); D.F. Jackson and C. Tranquille, Phys. Lett. **91A**, 324 (1982).
- ¹⁰V.I. Petrukhin and V.M. Suvorov, Zh. Eksp. Teor. Fiz. **70**, 1145 (1976); Sov. Phys. JETP **43**, 595 (1976).
- ¹¹V.A. Vasilyev, B.Lévay, A. Minkova, V.I. Petrukhin, and D. Horváth, Nucl. Phys. **A446**, 613 (1985).
- ¹²V.M. Bystritskii, V.A. Vasilyev, A.V. Zhelamkov, V.I. Petrukhin, V.E. Risin, V.M. Suvorov, B.A. Khomenko, and D. Horváth, in *Mesons in Matter*, Proc. Int. Symp., Dubna, 1977, Ed., V.N. Pokrovskii, p. 223.
- ¹³A.V. Bannikov, B. Lévay, V.I. Petrukhin, V.A. Vasilyev, L.M. Kochenda, A.A. Markov, V.I. Medvedev, G.L. Sokolov, I.I. Strakovsky, and D. Horváth, Nucl. Phys. **A403**, 515 (1983).
- ¹⁴G. Backenstoss, M. Izycki, W. Kowald, P. Weber, H.J. Weyer, S. Ljungfelt, U. Mankin, G. Schmidt, and H. Ullrich, Nucl. Phys. **A448**, 567 (1986).
- ¹⁵V.I. Petrukhin, V.E. Risin, and V.M. Suvorov, Yad. Fiz. **19**, 626 (1973); Sov. J. Nucl. Phys. **19**, 317 (1974).
- ¹⁶R.A. Naumann, and H. Daniel, Z. Phys. **A291**, 33 (1979).
- ¹⁷R. Bergmann, H. Daniel, T. von Egidy, F.J. Hartmann, J.J. Reidy, and W. Wilhelm, Phys. Rev. A **20**, 633 (1986).
- ¹⁸H. Daniel, F.J. Hartmann, R.A. Naumann, and J.J. Reidy, Phys. Rev. Lett. **56**, 448 (1986).
- ¹⁹C. Tranquille and D.F. Jackson, Phys. Rev. A **34**, 742 (1986).
- ²⁰J.R.H. Smith, A.S. Clough, D.F. Jackson, K.R. Smith, D.F. Measday, F. Entezami, A.J. Noble, S. Stanislaus, C.J. Virtue, M. Salomon, and K.A. Aniol, Proc. 6th Symp. on X- and γ -ray Sources and Applications, Ann Arbor, 1985; Nucl. Instr. Meth. **A242**, 465 (1986).
- ²¹D.F. Jackson and J.R.H. Smith, Phys. Rev. A **34**, 763 (1986).
- ²²V.I. Petrukhin, and Yu.D. Prokoshkin, Nucl. Phys. **54**, 414 (1964); V.I. Petrukhin, Yu.D. Prokoshkin, and A.I. Filippov, Yad. Fiz. **5**, 327 (1967); Sov. J. Nucl. Phys. **5**, 229 (1967).
- ²³J.F. Bartlett, J.R. Biel, D.B. Curtis, R.J. Dosen, T.D. Lagerhund, E.K. Quigg, D.J. Ritchie, and L.M. Taff, "FERMILAB MULTI computer program for data acquisition and analysis"; TRIUMF implementation by Y. Miles.
- ²⁴A.W. Bennett, A.K. Haynes, and J. Lloyd, "TRIUMF software package for off-line interactive data analysis".
- ²⁵F. James, and M. Roos, Comp. Phys. Comm. **10**, 343 (1975).

- ²⁶D. Horváth: Report KFKI-73-53, Budapest, 1973; Report JINR-10-12229, Dubna, 1979.
- ²⁷V.I. Petrukhin, V.E. Risin, I.F. Samenkova, and V.M. Suvorov, Zh. Eksp. Teor. Fiz. **69**, 1883 (1975); Sov. Phys. JETP **42**, 955 (1976).
- ²⁸W.H. Barkas, and M.J. Berger, In *Studies in penetration of charged particles in matter*, NAS-NRC 1134, 1964, p. 103.
- ²⁹M. Chabre, P. Depommier, J. Heintze, and V. Soergel, Phys. Lett. **5**, 67 (1963).
- ³⁰D. Bartlett, S. Devons, S.L. Meyer, and J.L. Rosen, Phys. Rev. B **136**, 1452 (1964).
- ³¹A.F. Dunaitsev, V.I. Petrukhin, and Yu.D. Prokoshkin, Nuovo Cimento **34**, 521 (1964).
- ³²M.E. Kost, Z.V. Krumstein, V.I. Mikheeva, L.N. Padurets, V.I. Petrukhin, V.M. Suvorov, A.A. Chertkov, and I.A. Yutlandov, Zh. Neorg. Khim. **21**, 1444 (1976); Russ. J. Inorg. Chem. **21**, 789 (1976).
- ³³A.K. Kachalkin, Z.V. Krumstein, A.P. Minkova, V.I. Petrukhin, V.M. Suvorov, D. Horváth, and I.A. Yutlandov, Zh. Eksp. Teor. Fiz. **77**, 26 (1979); Sov. Phys. JETP **50**, 12 (1979).
- ³⁴D. Horváth, A.V. Bannikov, A.K. Kachalkin, B. Lévy, V.I. Petrukhin, V.A. Vasilyev, I.A. Yutlandov, and I.I. Strakovsky, Chem. Phys. Lett. **87**, 504 (1982).
- ³⁵V.I. Goldanskii, N.N. Zatsepina, V.I. Petrukhin, V.E. Risin, V.M. Suvorov, I.F. Tupitsyn, N.I. Kholodov, and I.A. Yutlandov, Dokl. Akad. Nauk. SSSR **214**, 1337 (1974); Doklady Phys. Chem. **214**, 180 (1974).
- ³⁶L. Wilhelmova, P. Simrot, V.I. Petrukhin, V.E. Risin, L.M. Smirnova, V.M. Suvorov, and I.A. Yutlandov, Zh. Eksp. Teor. Fiz. **65**, 24 (1973); Sov. Phys. JETP **38**, 12 (1974).
- ³⁷V.I. Goldanskii, N.N. Zatsepina, V.I. Petrukhin, V.E. Risin, V.M. Suvorov, I.F. Tupitsyn, N.I. Kholodov, and I.A. Yutlandov, Dokl. Akad. Nauk. SSSR **214**, 1105 (1974); Doklady Phys. Chem. **214**, 149 (1974).
- ³⁸L. Pauling: *The Nature of the Chemical Bond* (Cornell Univ. Press, Ithaca, 1960).

Table I. The results of our experiment: Sample name, melting point, target thickness in carbon equivalent, number of π^0 's detected, and the measured relative pion capture probability in hydrogen. The capture probability W_T is normalised to CH_2 which is taken to be 12.9×10^{-3} .

Sample	M.P. (°C)	Δ_T (g/cm ² C)	N_{π^0}	W_T ($\times 10^{-3}$)
LiH	680	1.11, 1.56	14556	36.1 ± 1.3
CaH ₂	816	1.36	675	2.23 ± 0.10
NbH _{0.6}		2.10	86	0.024 ± 0.013
NbH _{0.9}		1.95	138	0.037 ± 0.013
SrH ₂	675	0.964	918	1.328 ± 0.048
Maleic anhydride	55	2.73	82	0.149 ± 0.022
Citraconic anhydride	7.5	1.05	268	0.662 ± 0.044
Succinic anhydride	119	1.76	827	0.737 ± 0.030
Methylsuccinic anhydride	34	1.05	1055	1.359 ± 0.045
Glutaric anhydride	52	1.85	1546	1.350 ± 0.041
3-methylglutaric anhydride	42	1.98	2676	2.185 ± 0.052
2,2-dimethylglutaric anhydride	36	2.02	2861	2.783 ± 0.058
3,3-dimethylglutaric anhydride	125	1.82	2635	2.785 ± 0.060
β -D-fructose (C ₆ O ₆ H ₁₂)	104	2.55	1828	1.845 ± 0.049
β -D-glucose (C ₆ O ₆ H ₁₂)	150	1.95	875	1.897 ± 0.072
D-(+)-mannose (C ₆ O ₆ H ₁₂)	132	1.48	636	1.729 ± 0.077
α -D-glucose (C ₆ O ₆ H ₁₂)	146	2.82	1486	1.614 ± 0.048
D-(+)-galactose (C ₆ O ₆ H ₁₂)	170	1.59	759	1.573 ± 0.067
D-(+)-xylose (C ₅ O ₅ H ₁₀)	91	1.46	669	1.807 ± 0.079
L-arabinose (C ₅ O ₅ H ₁₀)	160	1.92	663	1.668 ± 0.073
Oxalic acid (C ₂ O ₄ H ₂ ·2H ₂ O)	190	1.88	165	0.129 ± 0.016
Urea (H ₂ NCONH ₂)	134	3.23, 2.35	1103	1.334 ± 0.058
Uric acid	>300	1.48	91	0.172 ± 0.022
Melamine	>300	2.43	192	0.855 ± 0.046

Table II. The results of our experiment in comparison with previous results: Sample names and measured relative pion capture probabilities in hydrogen $W(\times 10^{-3})$.

Sample	$W_{\text{exp}}^{\text{present}}$	$W_{\text{exp}}^{\text{p. previous}}$	Ref.
LiH	36.1 ± 1.3	35 ± 4	32
CaH ₂	2.23 ± 0.10	2.5 ± 0.3	32
NbH _{0.9}	0.037 ± 0.013	0.38 ± 0.07	32

Table III. Fitting the anhydride results with a phenomenological model: Contributions of the various atomic components to the measured relative pion capture probability, with variable and fixed carbon contributions, all in units of 10^{-3} .

Component	Fit 1	Fit 2	Fit 3
C ₂ O ₃	1000. (reference)	1000. (reference)	1000. (reference)
C ^S	0.00 ± 1.60	1.60 (fixed)	20.0 (fixed)
C ^D	0.00 ± 28.7	28.7 (fixed)	20.0 (fixed)
H ⁰	0.0763 ± 0.0103	0.0823 ± 0.0113	0.0802 ± 0.0111
H ¹	0.1860 ± 0.0057	0.1877 ± 0.0059	0.1923 ± 0.0044
H ²	0.2978 ± 0.0069	0.2996 ± 0.0071	0.3280 ± 0.0065
H ³	0.3518 ± 0.0097	0.3542 ± 0.0099	0.3938 ± 0.0092
χ^2	9.18	10.52	11.22

Table IV. Fitting the anhydride results with a phenomenological model: Sample names, measured and calculated relative pion capture probabilities in hydrogen $W(\times 10^{-3})$.

Sample	Model composition	W_{exp}	W_{calc}	W_{calc}	W_{calc}
			Fit 1	Fit 2	Fit 3
Maleic	$1 + 2C^D + 2H^0$	0.149 ± 0.022	0.153	0.156	0.154
Citraconic	$1 + 2C^D + C^S + H^0 + 3H^1$	0.662 ± 0.044	0.634	0.609	0.619
Succinic	$1 + 2C^S + 46H^1$	0.737 ± 0.030	0.743	0.748	0.739
Methylsuccinic	$1 + 3C^S + 3H^1 + 3H^2$	1.359 ± 0.045	1.449	1.459	1.470
Glutaric	$1 + 3C^S + 4H^1 + 2H^2$	1.350 ± 0.041	1.338	1.342	1.343
3-methylglutaric	$1 + 4C^S + 4H^1 + H^2 + 3H^3$	2.185 ± 0.052	2.093	2.095	2.105
2,2-dimethylglutaric	$1 + 54C^S + 2H^1 + 8H^2$	2.783 ± 0.058	2.747	2.742	2.727
3,3-dimethylglutaric	$1 + 5C^S + 4H^1 + 6H^3$	2.785 ± 0.060	2.847	2.845	2.839

Figure captions

1. Contributory processes involved in pion capture in hydrogen in a Z-H molecule (Ref. 4).
2. Experimental set-up at TRIUMF. The fast π^- -mesons are slowed down in beam counters S_1 , S_2 , and S_3 , and a graphite wedge degrader D of variable thickness and then stop in the target. The stopping is checked by veto counter S_4 . The scintillators S_3 and S_4 are deuterated. The γ - γ coincidences from the π^0 decay were detected by two NaI spectrometers, TINA and MINA. The charged particles were separated using scintillation counters S_5 and S_6 , the neutrons by time of flight.
3. Range curve, i.e. π^0 -yield against degrader thickness measured in polyethylene. The smooth curve was obtained via least-squares fitting with function (11).
4. Time of flight to MINA against time of flight to TINA for neutral events. The sharp peak in the lower left corner represents the γ - γ coincidences, the broader peak to the right the neutrons. The box shows our TOF cut. Along the edges of the figure the projections are shown.
5. Energy spectra of neutral particles from π^- -mesons stopped in LiH as detected by TINA. (a) Neutrons and photons; (b) photons; (c) γ - γ coincidences.
6. Molecular structure of the organic samples.
7. Pion capture probability in hydrogen vs. melting point for sugar isomers. The straight line represents the function $W = 2.134 - 3.016 \times 10^{-3} \times MP$.

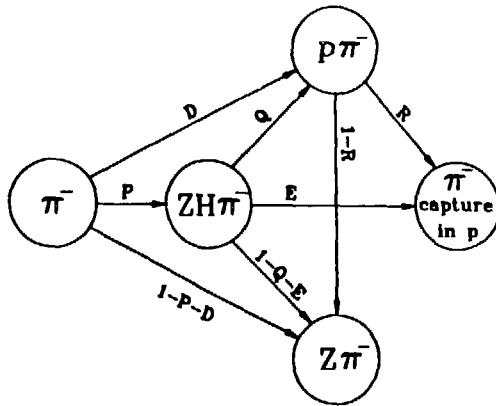


Fig. 1

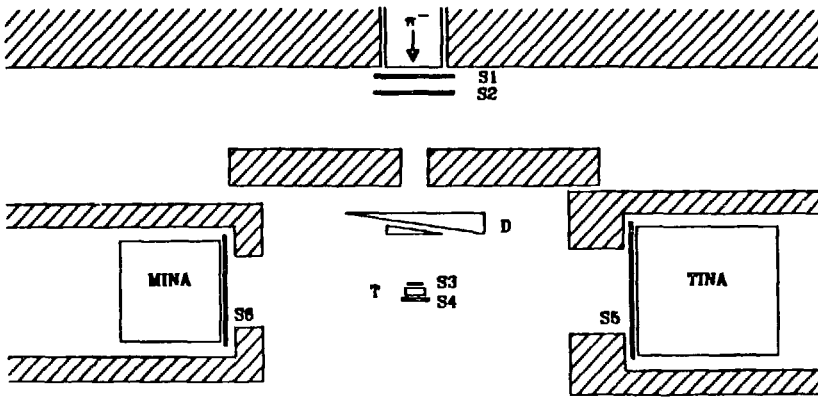


Fig. 2

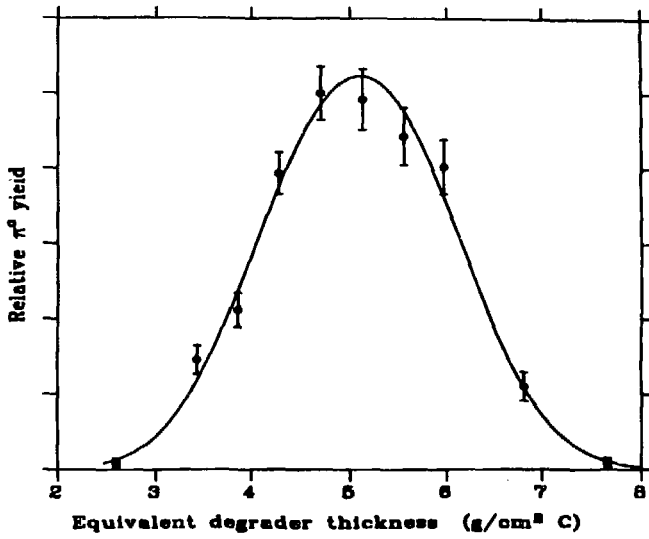


Fig. 3

Counts in arbitrary units

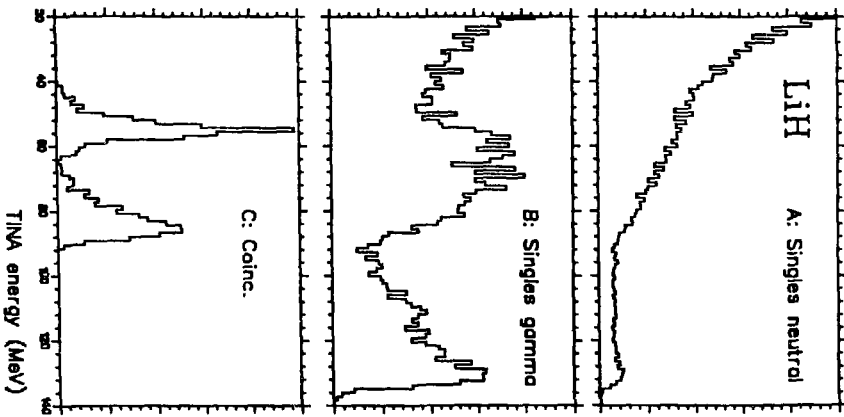


Fig. 5

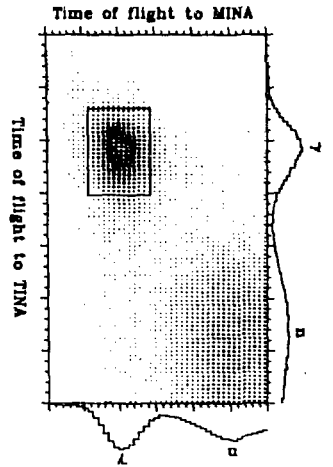


Fig. 4

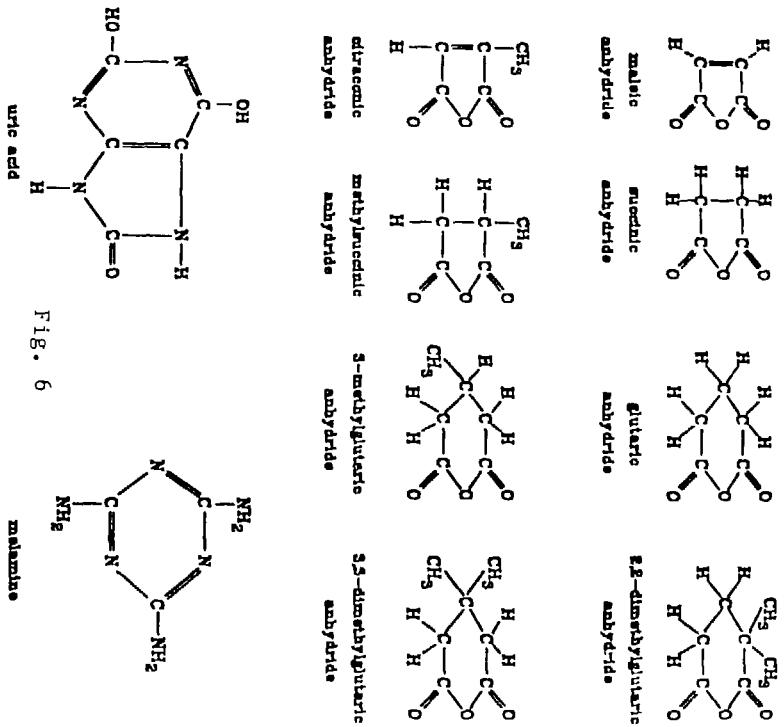


Fig. 6

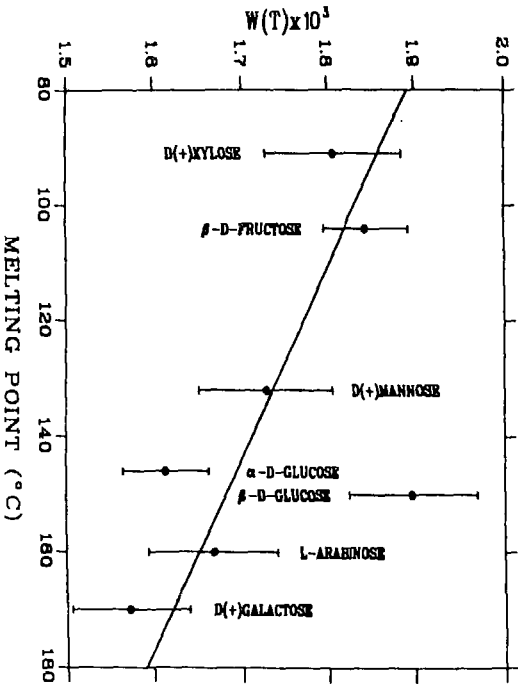


Fig. 7